IN-SITU SPECTROPHOTOMETRIC PROPERTIES FROM CHANG'E-4 ROVER MEASUREMENTS

TianYi Xu[1], YunZhao Wu[1, 2], [1]State Key Laboratory of Lunar and Planetary Sciences, Macau University of Science and Technology, Taipa, Macau, China (doroscope@foxmail.com), [2]Key Laboratory of Planetary Sciences, Purple Mountain Observatory, Chinese Academy of Sciences, Nanjing 210034, China.

Introduction: The Chang'E-4 (CE-4) lander and rover (Yutu-2) arrived at Von Kármán crater in the South Pole-Aitken Basin in January 3, 2019. During the 10th lunar workday of the mission, the VNIS spectrometer kept collecting data from two points for the purpose of photometric analysis, especially building photometric model with large-phase for photometric correction of large-phase data, such as Chang'E-4 data in the future. From September 23 to September 25, 2019, which is in the morning of the lunar day, the spectrometer stared at one point. These data were named from Site 68 to Site 78. From October 2 to October 4, which is in the afternoon of the lunar day, the spectrometer stared at another point. These data were named from Site 79 to Site 90. As the solar incidence direction changed during the process, the data can be good material for photometric studies.

The VNIS spectrometer consists of two parts: Visible and Near Infrared. The visible part has a wavelength range from 450nm to 945nm and provides 256×256 pixels image. The near infrared part has a wavelength range from 900nm to 2395nm and provides only one value for each band. The resolution of each part is 5nm. They are integrated into consideration in the processing.

Methods: The approximate true color images of the two points are shown in Figure 1. They are synthesized using the 475nm, 530nm, 700nm bands as blue, green and red respectively. The red circle represents the sampling region of near infrared values. So visible data in this region are averaged to match the near infrared data. After removing the gap and adjustment for abnormal jump [1], the reduced reflectance results, also known as IoF/LS, is shown in Figure 2 [2,3].

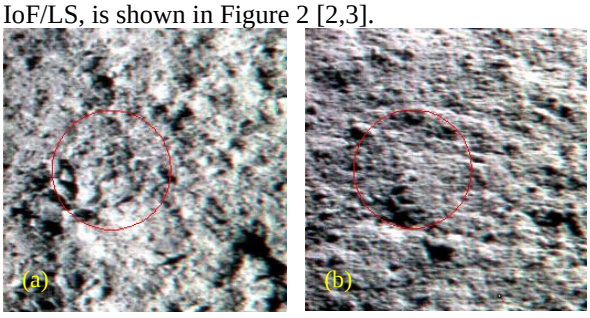

Fig. 1. (a) Color image of Site 78. (b) Site 79.

Nine bands were selected for photometric study. They include the 3 true color bands and 6 near infrared bands. As shown in Figure 3, by collecting the phase angle and reflectance of the sites, phase distribution consisting of points of different bands can be recognized. They behave differently due to the different basic reflectance. As the morning part contains wider range of phase angle and seems to behave more normally than the afternoon part, it is used for inversion here.

The phase data are used for Hapke model inversion here. The formula is written as Equation (1). Among the 9 free parameters, w, b, c, B_{S0}, h_S and θ are used for fitting [3-6]. The particle single scattering phase function p(g) is of the two-parameter Henyey-Greenstein expression, in Equation (2) [3-8]. To combat the problem of multiple-solution or ill-posed inverse and ensure physically meaningful inversion, A Monte-Carlo method developed in [9] was used for inversion in this study.

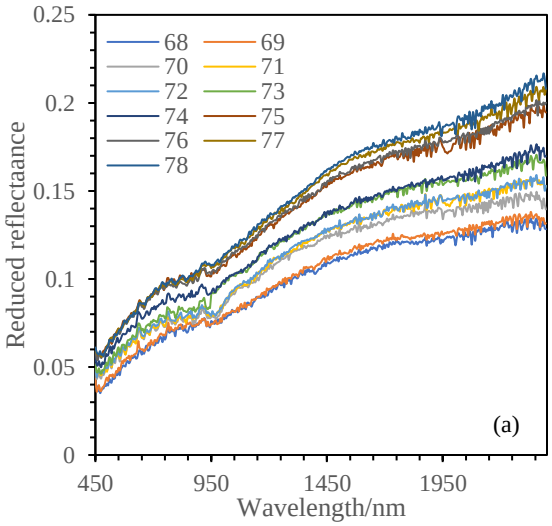

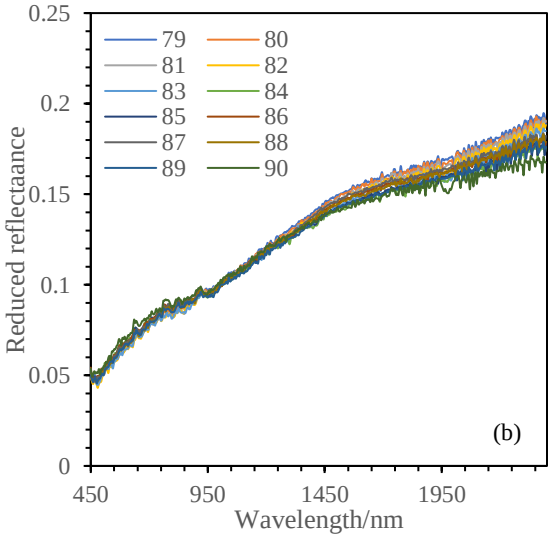

Fig. 2. Reduced reflectance of VNIS measurements. The label indicates different sites. (a) the lunar morning sites. (b) the lunar afternoon sites.

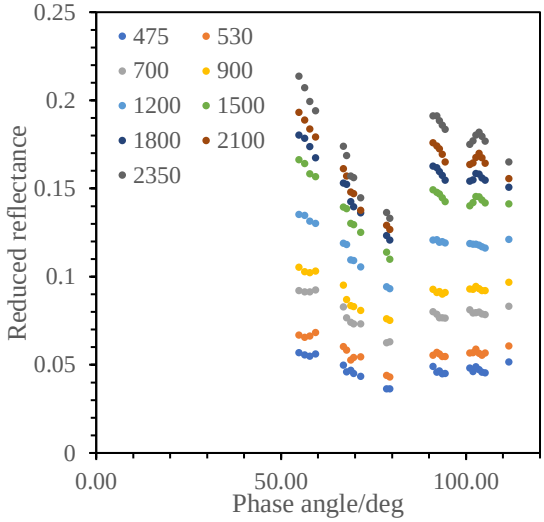

Fig. 3. Phase distribution of the selected 9 bands. The label indicates different wavelengths. They seem to be in two parts. The left part is the morning sites and the right part is the afternoon sites.

$$r_R = K\frac{w}{4}\left[p(g)\left(1 + B_{S0}B_S(g)\right) + M\right][1 + B_{C0}B_C(g)]S(i,e,\psi,\theta) \quad (1)$$

$$p(g) = \frac{1+c}{2}\frac{1-b^2}{(1-2bcos(g)+b^2)^{3/2}} + \frac{1-c}{2}\frac{1-b^2}{(1+2bcos(g)+b^2)^{3/2}} \quad (2)$$

Table 1. One group of best Hapke parameters solution inversed from lunar morning measurements using Monte-Carlo method.

λ/nm	w	h_S	b	c	B_{S0}
475	0.177	1.151	0.281	0.000	0.581
530	0.192	1.001	0.174	0.000	0.817
700	0.252	1.933	0.432	0.000	0.825
900	0.316	1.169	0.452	0.998	0.005
1200	0.373	1.067	0.464	0.000	0.811
1500	0.400	1.007	0.521	0.306	1.000
1800	0.441	1.026	0.536	0.249	1.000
2100	0.486	1.011	0.598	0.359	1.000
2350	0.517	1.046	0.626	0.585	1.000

Results: The results of Hapke parameters inversed from morning measurements are listed in Table 1. They are compared with the raw data in Figure 4. Because the phase angles are relatively high, far from the opposite effect region and there are few points in one group, parameters inversed can be unsteady and extreme, especially B_{S0} and h_S. According to [3,8,10], the relatively steady large parameter b at long wavelength may suggest relatively high symmetric characteristic of the regolith.

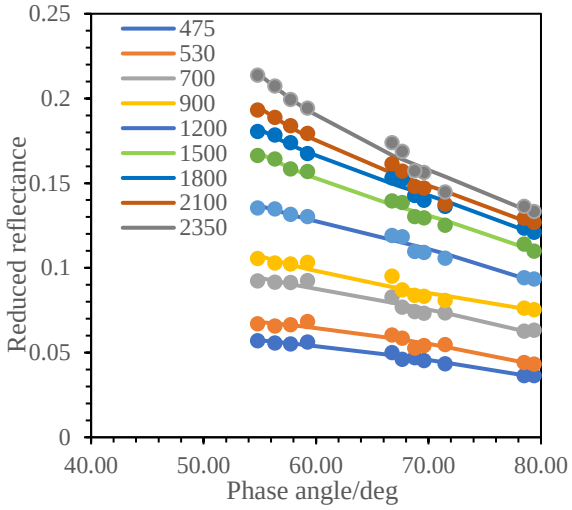

Fig. 4. Comparison of forward phase curve by the inversed parameters and raw phase distribution.

Conclusions: Here we analyzed the spectrophotometric properties of regolith based on Chang'E-4 VNIS spectrometer data. By reversing using Hapke model, we obtained the Hapke parameters of different bands and inferred the photometric properties of regolith. The regolith appears to have relatively high symmetric characteristic. Also, the measurements of the VNIS were at large emission and phase angles, can complement existing measurements for the range of photometric geometry. The large-phase model built in this study can be used for photometric correction of data with large phase angle such as Chang'E-3 and Chang'E-4 and others..

Acknowledgements: This research was supported by the Macau Science and Technology Development Fund (0042/2018/A2), and Minor Planet Foundation of Purple Mountain Observatory.

References:[1] Wu Y. et al. (2018) *Astron. J. 155(5)*, 213. [2] Thuillier G. et al. (2004) *Advan. Space Res. 34(2)*, 256-261. [3] Hapke, B. (2012) *Cambridge university press.* [4] Sato, H. et al. (2014). *J. Geophys. Res.: Planets*, *119*(8), 1775-1805. [5] Hapke, B. (2012). *Icarus*, *221*(2), 1079-1083. [6] Hapke, B., & Sato, H. (2016). *Icarus*, *273*, 75-83. [7] Shepard, M. K., & Helfenstein, P. (2007). *J. Geophys. Res.: Planets*, *112*(E3). [8] McGuire, A. F., & Hapke, B. W. (1995). *Icarus*, *113*(1), 134-155. [9] Wu, Y. et al. (2009). *Remote Sensing of Envir.*, *113*(1), 213-223. [10] Johnson, J. R. et al. (2013). *Icarus*, *223*(1), 383-406.